1521-0111/84/4/630–642$25.00
MOLECULAR PHARMACOLOGY

http://dx.doi.org/10.1124/mol.113.087072
Mol Pharmacol 84:630–642, October 2013

Fluorescence Correlation Spectroscopy Analysis of Serotonin, Adrenergic, Muscarinic, and Dopamine Receptor Dimerization: The Oligomer Number Puzzle

Katharine Herrick-Davis, Ellinor Grinde, Ann Cowan, and Joseph E. Mazurkiewicz

Center for Neuropharmacology and Neuroscience, Albany Medical College, Albany, New York (K.H.-D., E.G., J.E.M.); and Center for Cell Analysis and Modeling, University of Connecticut Health Center, Farmington, Connecticut (A.C.)

Received May 2, 2013; accepted August 1, 2013

ABSTRACT

The issue of G protein–coupled receptor (GPCR) oligomer status has not been resolved. Although many studies have provided evidence in favor of receptor-receptor interactions, there is no consensus as to the exact oligomer size of class A GPCRs. Previous studies have reported monomers, dimers, tetramers, and higher-order oligomers. In the present study, this issue was examined using fluorescence correlation spectroscopy (FCS) with photon counting histogram (PCH) analysis, a sensitive method for monitoring diffusion and oligomer size of plasma membrane proteins. Six different class A GPCRs were selected from the serotonin (5-HT_{2A}), adrenergic (α_{1b}-AR and β_2-AR), muscarinic (M_1 and M_2), and dopamine (D_1) receptor families. Each GPCR was C-terminally labeled with green fluorescent protein (GFP) or yellow fluorescent protein (YFP) and expressed in human embryonic kidney 293 cells. FCS provided plasma membrane diffusion coefficients on the order of 7.5×10^{-9} cm^2/s. PCH molecular brightness analysis was used to determine the GPCR oligomer size. Known monomeric (CD-86) and dimeric (CD-28) receptors with GFP and YFP tags were used as controls to determine the molecular brightness of monomers and dimers. PCH analysis of fluorescence-tagged GPCRs revealed molecular brightness values that were twice the monomeric controls and similar to the dimeric controls. Reduced χ^2 analyses of the PCH data best fit a model for a homogeneous population of homodimers, without tetramers or higher-order oligomers. The homodimer configuration was unaltered by agonist treatment and was stable over a 10-fold range of receptor expression level. The results of this study demonstrate that biogenic amine receptors freely diffusing within the plasma membrane are predominantly homodimers.

Introduction

G protein–coupled receptors (GPCRs) represent one of the largest families of plasma membrane-associated receptors. They are present on virtually every cell in the human body and regulate a wide variety of physiologic responses to light, odorants, hormones, neurotransmitters, and therapeutic agents. Physiologic processes regulated by GPCR activation and blockade have been studied for decades, but there is still great debate as to what constitutes the functional signaling unit: Is it a monomer, dimer, or higher-order oligomer? Although monomeric GPCRs in reconstituted lipid vesicles can activate G proteins (Whorton et al., 2007), GPCR dimers/oligomers have been reported in native tissues and primary cultures (Fotiadis et al., 2003; Rashid et al., 2007; Albizu et al., 2010; Herrick-Davis et al., 2012; Knepp et al., 2012; Teitler and Klein, 2012; Jastrzebska et al., 2013). Although the functional significance of class A GPCR dimerization is still a subject of great debate, GPCR homodimerization and heterodimerization have been reported to regulate ligand binding, second messenger activation, and receptor trafficking (reviewed in Milligan, 2013).

For class A GPCRs, there is no consensus in the published literature as to their monomer/oligomer status. Quantitative studies designed to determine the monomeric/oligomeric composition of class A GPCRs have reported the presence of monomers (James et al., 2006; Meyer et al., 2006; Dorsch et al., 2009; Hern et al., 2010; Kasai et al., 2011), dimers (Mercier et al., 2002; Canals et al., 2004; Goin and Nathanson, 2006; Harikumar et al., 2008; Dorsch et al., 2009; Herrick-Davis et al., 2012; Knepp et al., 2012; Teitler and Klein, 2012; Patowary et al., 2013), tetramers (Fung et al., 2009; Pisterzi et al., 2010; Patowary et al., 2013), and higher-order oligomers (Guo et al., 2008; Dorsch et al., 2009; Albizu et al., 2010; O'Dowd et al., 2011). Coimmunoprecipitation, resonance energy transfer (RET), fluorescence lifetime imaging (FLIM), and bimolecular fluorescence complementation (BiFC) are commonly used methods to evaluate protein–protein interactions. However, immunoprecipitation requires solubilization and disruption of the native GPCR plasma membrane

This work was supported by the National Institutes of Health National Institute of Mental Health [Grant R21-MH086796 (to K.H.-D.)].
dx.doi.org/10.1124/mol.113.087072.

ABBREVIATIONS: 2D, two-dimensional; 3D, three-dimensional; AR, adrenergic receptor; BiFC, bimolecular fluorescence complementation; CPSM, counts per second per molecule; C-YFP, C-terminal half of yellow fluorescent protein; FCS, fluorescence correlation spectroscopy; FLIM, fluorescence lifetime imaging; FRAP, fluorescence recovery after photobleach; GFP, green fluorescent protein; GPCR, G protein–coupled receptor; MEM, minimal essential medium; N-YFP, N-terminal half of yellow fluorescent protein; PCH, photon counting histogram; PSF, point spread function; RET, resonance energy transfer; TIRF, total internal reflection fluorescence; YFP, yellow fluorescent protein.

environment, and RET and BiFC are proximity-based assays that monitor the distance between the fluorescent probes. Although these methods can provide evidence consistent with the hypothesis that GPCRs form dimers/oligomers, they do not provide conclusive proof of protein–protein interactions. Recently, purification of photoactivated rhodopsin from native disc membranes using lauryl-maltose-neopentyl-glycol and three-dimensional (3D) projection analysis revealed a rhodopsin dimer in complex with a single G protein (Jastrzebska et al., 2013).

Fluorescence correlation spectroscopy (FCS) provides a good alternative for investigating diffusion and protein interactions in living cells. It requires very low protein expression levels, making it suitable for studying plasma membrane GPCRs at physiologic expression levels. FCS records the fluctuations in fluorescence intensity arising from individual fluorescent molecules, in a temporal manner (Magde et al., 1972). Combining confocal microscopy with FCS led to the development of sensitive methods for monitoring protein dynamics in living cells (Qian and Elson, 1991; Rigler et al., 1993; Pramanik et al., 2001; Digman et al., 2005). FCS has been used to monitor diffusion and ligand binding for ion channels, tyrosine kinase receptors, and GPCRs (reviewed in Briddon and Hill, 2007), to examine neuropeptide Y and β-arrestin interactions (Kilpatrick et al., 2012), and to monitor the oligomer status of various receptors including somatostatin (Patel et al., 2002), epidermal growth factor (Liu et al., 2007), ciliary neurotrophic factor (Neugart et al., 2009), estrogen (Savatier et al., 2010), and serotonin 5-HT_{1A} (Ganguly and Chattopadhyay, 2010) and 5-HT_{2C} receptors (Herrick-Davis et al., 2012).

The oligomer status of a protein cluster can be determined by analyzing the amplitude of the fluctuations in fluorescence intensity measured in an FCS experiment. A photon counting histogram (PCH) can be generated from the FCS data and used to determine the molecular brightness of a fluorescence-tagged protein (Chen et al., 1999). Since the molecular brightness of a cluster of fluorescent molecules is directly proportional to the number of fluorescent molecules present in the cluster, the molecular brightness provides an estimate of the number of fluorescent molecules within the protein complex. Molecular brightness analysis has been used to explore the oligomeric status of nuclear retinoid X receptors (Chen et al., 2003), epidermal growth factor receptors (Saffarian et al., 2007), urokinase plasminogen activator receptors (Malengo et al., 2008), and serotonin 5-HT_{2C} receptors (Herrick-Davis et al., 2012).

FCS combined with confocal microscopy and PCH provide powerful methods for determining the molecular brightness of individual fluorescence-tagged proteins as a measure of their oligomer size. The present study describes the application of FCS and PCH analysis for determining the oligomeric size of biogenic amine serotonin (5-HT_{2A}), adrenergic (α_{1b}-AR and β_2-AR), muscarinic (M_1 and M_2), and dopamine (D_1) receptors freely diffusing within the plasma membrane of living cells.

Materials and Methods

Plasmids. cDNAs encoding the 5-HT_{2A}, α_{1b}-AR, β_2-AR, M_1-muscarinic, M_2-muscarinic, and D_1-dopamine receptors were polymerase chain reaction–amplified from human total genomic DNA and cloned into the pEGFP-N1 and pEYFP-N1 vectors (Clonetech Laboratories, Mountain View, CA) at EcoRI/BamHI to create chimeric receptors with fluorescent tags on the C terminus of the receptor. Site-directed mutagenesis (Stratagene, La Jolla, CA) was used to create an A206K mutation in all green fluorescent protein (GFP) constructs and an L221K mutation in the monomeric yellow fluorescent protein (YFP) and dimeric CD-28/YFP constructs to eliminate potential aggregation of the fluorescent tags (Zacharias et al., 2002). BiFC pairs, N- and C-terminal half of yellow fluorescent protein (N-YFP and C-YFP, respectively), were made by site-directed mutagenesis using the β_2-AR/YFP cDNA as the starting template. β_2-AR/N-YFP was made by inserting a stop codon at amino acid 156 of YFP. β_2-AR/C-YFP was made by inserting a BamHI site at amino acid 156 of the YFP, followed by BamHI digest to remove amino acids 1–155 of the YFP, and subsequent re-ligation. The A_{2a}-adenosine BiFC constructs were generously provided by S. Briddon (University of Nottingham). CD-28/YFP was a generous gift from J. Miller (University of Rochester). CD-86/GFP and CD-86/GFP-GFP were generously provided by G. Milligan (University of Glasgow).

Cell Culture, Transfection, and Drug Treatment. Human embryonic kidney (HEK) 293 cells (American Type Culture Collection, Manassas, VA) were cultured in Dulbecco's minimal essential medium (Cellgro, Manassas, VA) with 10% fetal bovine serum (HyClone, Logan, UT) in a humidified chamber at 37°C, 5% CO_2. HEK293 cells were plated in 6-well plates fitted with 25-mm poly-D-lysine coated glass coverslips (Thermo Fisher Scientific, Waltham, MA) at a density of 5×10^5 cells per coverslip and transfected with 50 ng of the indicated plasmid DNA using lipofectamine reagent (Invitrogen, Carlsbad, CA) for 5 hours. After transfection, cells were cultured in minimal essential medium (MEM) (without phenol red) with 10% charcoal stripped serum (Gibco, Carlsbad, CA) for 20 hours at 37°C, 5% CO_2. In our hands, this transfection protocol typically yields plasma membrane receptor expression levels on the order of 1 pmol/mg protein, by radioligand binding analysis. For drug treatment, isoproterenol and carbachol were diluted in HEPES-buffered MEM (without phenol red) and added directly to the viewing chamber to achieve a final concentration of 0.1 μM. FCS measurements were initiated 1 minute after the addition of ligand. We previously determined this time point to be sufficient for receptor activation, measured as β-arrestin recruitment to the plasma membrane (Herrick-Davis et al., 2007, 2012).

FCS. For FCS measurements, cells were washed twice with HEPES-buffered Krebs-ringer (without glucose) and the coverslip was placed in a viewing chamber with 1 ml HEPES-buffered MEM (without phenol red). FCS measurements were made using a Zeiss LSM-780 confocal microscope equipped with gallium arsenide phosphide photon detectors (Carl Zeiss, Jena, Germany). One-photon excitation with a continuous argon ion laser was performed using a 40× (numerical aperture 1.2) C-apochromat water immersion objective to create an observation volume on the order of 10^{-15} liters. Since the observation volume is not illuminated homogenously, optimal positioning of the plasma membrane within the center of the observation volume is critical for accurate determination of the molecular brightness of fluorescent-tagged membrane proteins. FCS measurements were made on the apical plasma membrane, directly above the cell nucleus of HEK293 cells transfected with the indicated fluorescence-tagged receptor. Positioning of the plasma membrane in the center of the observation volume was achieved by monitoring the photon counts per molecule in real time (by opening the interactive counts/molecule window in the Zeiss software menu) while simultaneously focusing upward through the plasma membrane to identify the focal plane corresponding to the maximal photon counts per molecule. FCS measurements were recorded at 23°C in HEPES-buffered MEM (without phenol red) for 100 seconds, as 10 consecutive 10-second intervals. As fluorescent-tagged receptors enter and diffuse through the observation volume they are excited by the laser. GFP and YFP were excited at 488 and 514 nm, respectively, with a laser intensity of 0.1%. It is critical to use the lowest laser power possible, while still maintaining a good signal to noise ratio, because higher

laser powers will result in photobleaching of the fluorescent probe. The time-dependent fluctuations in fluorescence intensity were recorded on gallium arsenide phosphide detectors as follows: emitted fluorescence captured by the objective is passed through an appropriate band pass filter and focused onto the detector using a pinhole of one airy unit. FCS recordings were analyzed by a digital temporal correlator (using nonlinear least-squares minimization; Zeiss Aim 4.2 software) to calculate the autocorrelation function $G(\tau)$, which represents the time-dependent decay in fluorescence fluctuation intensity as in Eq. 1,

$$G(\tau) = \frac{<\delta F(t)\cdot\delta F(t+\tau)>}{<F(t)>^2} \quad (1)$$

where $G(\tau)$ is the <time average> of the change in fluorescence fluctuation intensity (δF) at some time point (t) and at a time interval later ($t + \tau$), divided by the square of the average fluorescence intensity. Autocorrelation analyses were performed using the Zeiss Aim 4.2 software package with an autocorrelation bin time of 0.2 μs. FCS data were fit to a two-dimensional (2D) model (for lateral diffusion within the plasma membrane) with two components as in Eq. 2,

$$G(\tau) = 1 + AN^{-1}[F_1(1+{}^{\tau}/_{\tau_{D1}})^{-1} + F_2(1+{}^{\tau}/_{\tau_{D2}})^{-1}] \quad (2)$$

where N is the number of molecules in the observation volume. F_1 and F_2 as well as τ_{D1} and τ_{D2} represent the respective fractions and diffusion times of the two components. A pre-exponential term is included to account for photophysical properties (blinking) of the fluorescent probe $\left\{A = 1 + \left(T_b e^{-\frac{\tau}{\tau_b}}\right)(1-T_b)^{-1}\right\}$, where T_b and τ_b represent the blinking fraction and relaxation time, respectively. It should be noted that individual GFP and YFP molecules are not always fluorescent. They can exhibit blinking, exist in a prolonged dark state, or be immature and nonfluorescent (Ulbrich and Isacoff, 2007). The resulting autocorrelation curve depicts the fluorescence intensity fluctuations as a function of particle number and diffusion time. The average dwell time of the fluorescent species within the observation volume (τ_D) is calculated from the mid-point of the autocorrelation curve. The diffusion coefficient (D) for lateral diffusion of fluorescence-tagged GPCRs within the plasma membrane can then be calculated as in Eq. 3, where ω_0 is the radial waist of the observation volume.

$$D = \frac{\omega_o^2}{4\tau_D} \quad (3)$$

The radial waist was determined experimentally from the full width at half maximum of a Gaussian distribution fitted to the image of subresolution fluorescent beads (0.1 μm, FluoSpheres; Invitrogen) as described by Cole et al. (2011). In our experimental set-up, the radial waist was determined to be 0.30 μm.

The amplitude of the autocorrelation function $G(0)$ (equal to the y-intercept) is inversely related to the number of molecules in the observation volume (N_{PSF}) as in Eq. 4,

$$N_{PSF} = \frac{1}{G(0)-1}\cdot\gamma \quad (4)$$

where γ is the point spread function (PSF) that describes the shape of the observation volume. The numerical value of γ differs depending on the model selected for analysis and is 0.5 for 2D FCS analysis and 0.35 for a 3D Gaussian model used for PCH analysis. Although the absolute numerical values of molecular brightness will vary depending on whether a 2D FCS or 3D PCH model is selected (due to the different numerical value of γ used in Eq. 4), the overall conclusions will remain the same, because the molecular brightness of a dimer will still be twice that of a monomer regardless of the selected model.

The average fluorescence intensity or average photon count rate (k) recorded for a given sample is determined by the number of fluorescent molecules (N_{PSF}) and their molecular brightness (ε), as described in Eq. 5.

$$k = N_{PSF}\cdot\varepsilon \quad (5)$$

Thus, dividing the count rate (k) by the number of molecules (N_{PSF}) provides an estimate of the molecular brightness (ε) of the sample.

PCH. Fluorescence fluctuation data recorded during an FCS experiment can be used to generate PCHs, which provide quantitative information about the number of fluorescent molecules and the number of photon counts per molecule (Chen et al., 1999). PCH analysis uses a 3D Gaussian approximation of the laser beam profile. In the present study, cells transfected with fluorescence-tagged receptors were selected with an average plasma membrane photon count rate ranging from 50 to 250 kHz, corresponding to plasma membrane receptor expression levels in the nanomolar range. Membrane regions containing ruffles, filopodia, and high concentrations of fluorescent proteins (>250 kHz) were avoided. Ten measurements were made on the upper plasma membrane of each cell by monitoring the photon count rate for 100 seconds, as 10 consecutive 10-second observation periods. While the laser intensity was set to 0.1% to minimize photobleaching, photobleaching was apparent during the first 10-second observation period. Therefore, the average molecular brightness from the second through tenth observation periods was calculated and reported as the molecular brightness for that cell. Segments of the fluorescence intensity trace that showed large spikes or drifts in fluorescence intensity (due to cell movement) were excluded from the analysis. To generate a histogram, each 10-second observation period was broken down into 1 million intervals or bins (PCH bin time = 10 μs). Histograms were constructed using the PCH module in the Zeiss Aim 4.2 software in which the number of 10-μs bins was plotted on the y-axis and photon counts on the x-axis. The resulting histogram depicts the number of bins that registered 1,2,3 photon counts and so forth during one 10-second observation period. Since a constant intensity light source produces a photon count distribution that follows Poisson statistics, as fluorescent molecules enter and diffuse through the nonhomogenously illuminated observation volume, the fluctuations in fluorescence intensity result in a broadening of the Poisson distribution. This super-Poisson characteristic is observed in the tail of the PCH curve. Initially, PCH data were fit to a one-component model in which concentration and molecular brightness were allowed to be free (and the first-order correction was fixed at zero) to determine the average molecular brightness of the sample.

Multicomponent PCH Analysis. The PCH data were subjected to a multicomponent analysis to test for the presence of a mixture of monomers, dimers, and tetramers. Fitting the PCH data to a multicomponent model was performed as described by Müller et al. (2000) using the PCH module in the Zeiss Aim4.2 analysis software. Molecular brightness values were fixed based on the control values for monomers and dimers obtained from the initial one-component fit of the data (Table 1). Reduced χ^2 analysis was used to determine the goodness of fit to both one-component and multicomponent models.

Controls for Molecular Brightness Analysis. Five different plasma membrane controls were used to decode the molecular brightness of GFP- and YFP-tagged biogenic amine receptors. Known monomeric (CD-86) and dimeric (CD-28) plasma membrane receptors with C-terminal GFP (CD-86/GFP and CD-86/GFP-GFP) and YFP (CD-28/YFP) were used to determine the molecular brightness of GFP and YFP monomers and dimers. The β_2-AR/YFP BiFC pair and co-expression of β_2-AR/GFP or M_1/GFP with a 3-fold excess of untagged, nonfluorescent receptors were used as additional controls. To eliminate self-aggregation of GFP or YFP (Zacharias et al., 2002), all GFP constructs contained an A206K mutation and the CD-28/YFP construct contained an L221K mutation. To determine the contribution of background autofluorescence from cytoplasmic proteins, a dilute

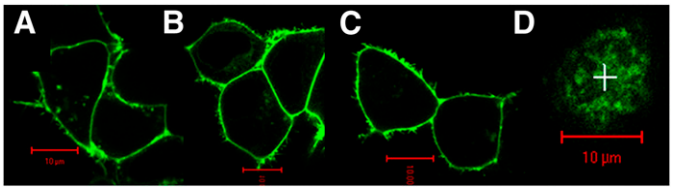

Fig. 1. Confocal microscopy of transfected HEK293 cells showing plasma membrane localization of YFP-tagged proteins. (A) β_2-AR/YFP. (B) D_1/YFP. (C) Dimeric CD-28/YFP. (D) The upper plasma membrane of an HEK293 cell expressing β_2-AR/YFP showing the location (marked by +) where an FCS recording was made. Red scale bar, 10 μm.

solution of purified monomeric GFP was evaluated. The molecular brightness of GFP in solution [8268 counts per second per molecule (CPSM)] was similar to GFP from pEGFP plasmid expressed in the cytosol of HEK293 cells (8508 CPSM), indicating that background autofluorescence from cytoplasmic proteins was minimal (approximately 3%) in our experimental set-up.

2D FCS Analysis of Molecular Brightness with Varying Receptor Expression Levels. To investigate the relationship between molecular brightness and receptor expression level, 2D FCS analysis was used to determine the number of fluorescent molecules in the observation volume (as in Eq. 4) and the molecular brightness (as in Eq. 5). The area of plasma membrane in the observation volume was calculated using $\pi\omega_0^2$, where ω_0 is the radius of the observation volume (0.30 μm), determined experimentally as described in Eq. 3. The total surface area of an HEK293 cell, determined to be 2591 μm^2 (Sommerhage et al., 2008), was used to estimate the total number of receptors per cell.

Results

FCS and PCH analyses were applied to determine the diffusion dynamics and oligomer status of biogenic amine GPCRs selected from the serotonin (5-HT_{2A}), adrenergic (α_{1b}-AR and β_2-AR), muscarinic (M_1 and M_2), and dopamine (D_1) receptor families. Fluorescent probes (GFP or YFP) were attached to the C terminus of each GPCR. In the present study, proper plasma membrane targeting of fluorescence-tagged GPCRs was confirmed by confocal microscopy (Fig. 1). FCS

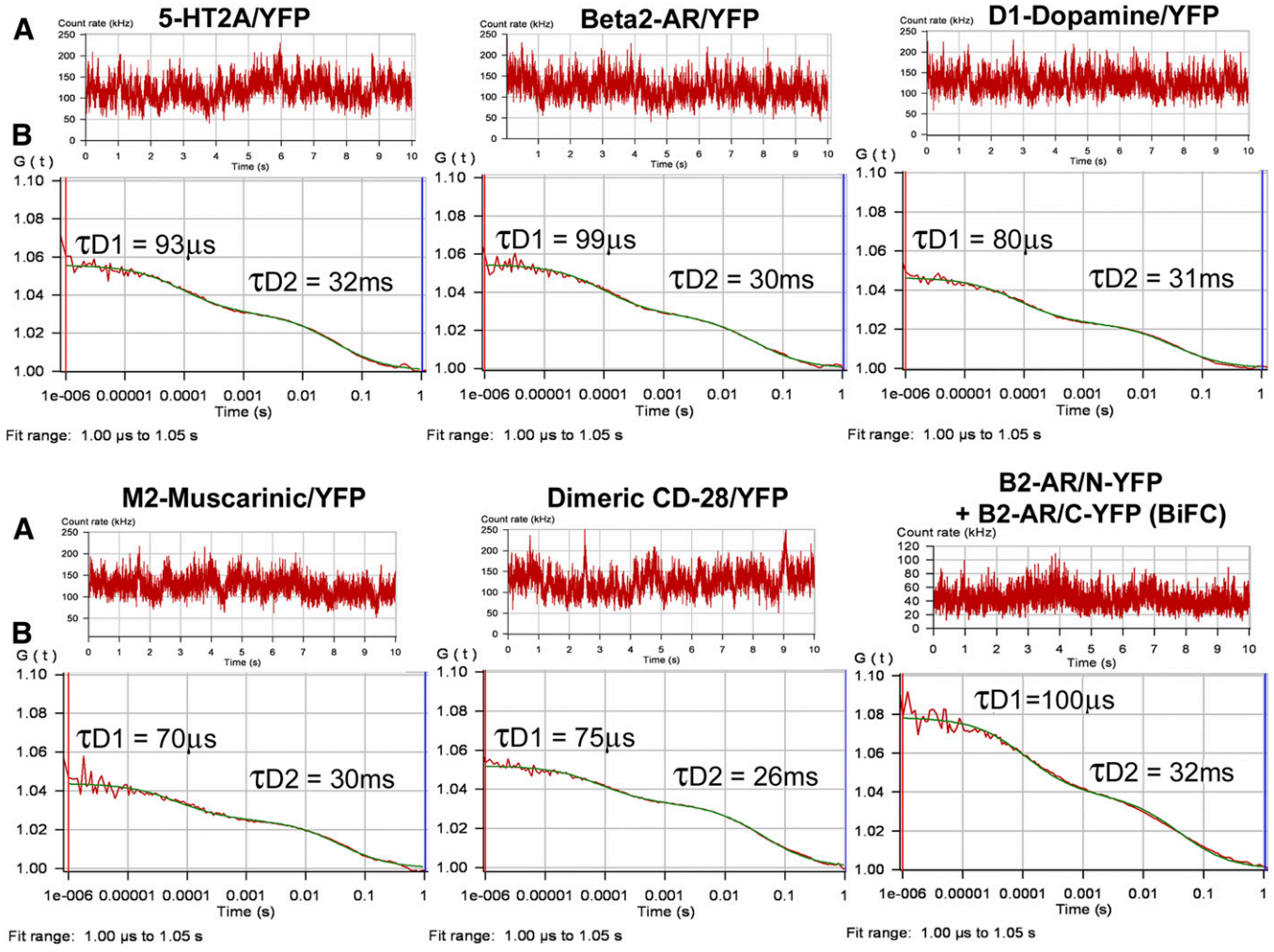

Fig. 2. FCS recordings from the plasma membrane of HEK293 cells expressing YFP-tagged GPCRs. (A) Fluorescence intensity traces for one 10-second observation period. (B) Autocorrelation analysis of the fluorescence intensity traces. The red line represents the autocorrelation of the observed fluorescence signal and the green line represents the fit to a two-component model. The fast component (measured in microseconds) is related to the photophysical properties of the fluorescent probe, whereas the slower component (measured in milliseconds) represents the translational diffusion of fluorescence-tagged receptors in the plasma membrane. Dividing the average photon count rate (kHz) determined from the fluorescence intensity trace shown in A by the number of fluorescent molecules determined from the autocorrelation curve shown in B (calculated as in Eq. 4) predicts the average molecular brightness of the sample expressed as CPSM.

TABLE 1

FCS and PCH analysis of HEK293 cells expressing YFP- and GFP-tagged biogenic amine receptors

Known monomeric (CD-86) and dimeric (CD-28) receptors are included as controls. M_1/GFP and β_2-AR/GFP were coexpressed with a 3-fold excess of untagged/nonfluorescent receptors (e.g., M_1/GFP + M_1/no tag 1:3). FCS τ_{D2} values for GPCR diffusion within the plasma membrane are reported in milliseconds and represent the average dwell time of the receptor in the observation volume. Diffusion coefficients ($\mu m^2/s$) were calculated using Eq. 3 (in the *Materials and Methods*). The 2D FCS molecular brightness values were determined by dividing the photon count rate by the number of molecules (as in Eqs. 4 and 5 in the *Materials and Methods*). The 3D PCH analysis was performed using the PCH module in the Zeiss Aim 4.2 software package by fitting the data to a one-component model (for a single population of fluorescent species) and the resulting reduced χ^2 values are reported. Data represent the mean ± S.E.M. for the number of cells as indicated.

Fluorescent Receptor	Diffusion		Molecular Brightness		Reduced χ^2	n
			2D FCS	3D PCH		
	ms	$\mu m^2/s$				
Dimeric CD-28/YFP	29.1 ± 1.7	0.77 ± 0.03	12,728 ± 372	17,819 ± 484	1.07 ± 0.08	20
5-HT_{2A}/YFP	31.1 ± 0.6	0.72 ± 0.01	12,714 ± 255	17,927 ± 332	1.13 ± 0.04	25
α_{1b}-AR/YFP	32.5 ± 0.6	0.69 ± 0.02	12,560 ± 606	17,709 ± 849	1.37 ± 0.13	15
D_1/YFP	30.8 ± 0.6	0.73 ± 0.01	12,716 ± 509	17,930 ± 712	1.07 ± 0.04	15
M_2/YFP	30.1 ± 0.5	0.75 ± 0.01	13,295 ± 410	18,480 ± 578	1.06 ± 0.07	10
β_2-AR/YFP	30.3 ± 1.4	0.74 ± 0.03	13,201 ± 866	18,279 ± 1311	1.11 ± 0.10	12
β_2-AR/YFP BiFC	31.3 ± 1.1	0.72 ± 0.02	6854 ± 343	9596 ± 480	1.10 ± 0.06	13
Monomeric CD-86/GFP	32.7 ± 1.4	0.69 ± 0.03	7088 ± 135	9364 ± 390	1.04 ± 0.10	12
CD-86/GFP-GFP	32.5 ± 1.1	0.69 ± 0.02	13,131 ± 450	18,777 ± 565	1.19 ± 0.08	10
M_1/GFP	33.7 ± 2.1	0.67 ± 0.04	12,594 ± 295	17,852 ± 410	1.04 ± 0.06	20
M_1/GFP + carbachol	36.0 ± 2.0	0.63 ± 0.04	12,878 ± 390	18,029 ± 546	1.12 ± 0.08	10
M_1/GFP + M_1/no tag (1:3)	36.5 ± 0.9	0.62 ± 0.02	6980 ± 334	9912 ± 434	1.08 ± 0.08	10
β_2-AR/GFP	32.1 ± 1.0	0.70 ± 0.02	12,558 ± 572	18,117 ± 790	1.23 ± 0.05	15
β_2-AR/GFP + isoproterenol	37.8 ± 1.7	0.60 ± 0.03	12,681 ± 564	17,602 ± 369	1.12 ± 0.09	12
β_2-AR/GFP + β_2-AR/no tag (1:3)	32.0 ± 1.1	0.70 ± 0.02	7087 ± 216	10,564 ± 300	1.05 ± 0.05	13
β_2-AR/GFP + M_1/no tag (1:3)	35.2 ± 1.7	0.63 ± 0.03	12,506 ± 227	17,950 ± 351	1.11 ± 0.09	10

measurements were made on the upper plasma membrane of transfected HEK293 cells (as shown in Fig. 1D).

In an FCS experiment, a high numerical aperture objective is used to focus a laser beam into a small diffraction-limited spot, creating a detection or observation volume on the order of 10^{-15} liters. The upper plasma membrane of HEK293 cells expressing fluorescence-tagged GPCRs was positioned within the laser-illuminated observation volume by focusing upward from the middle of the cell to the top, while simultaneously monitoring the photon counts per molecule. Optimal positioning of the plasma membrane within the center of the observation volume is critical for accurate FCS/PCH analysis of molecular brightness because the detected photon counts decrease as fluorescent molecules travel away from the center of the observation volume. The fluorescence-tagged GPCRs, freely diffusing within the plasma membrane, pass through the observation volume where they are excited by a laser and give off bursts of photons. The fluctuations in fluorescence, produced by fluorescence-tagged GPCRs entering and leaving the observation volume, are recorded in real time, as shown in the fluorescence intensity traces in Fig. 2A.

Autocorrelation analyses of the fluorescence intensity traces (from Fig. 2A) are performed using a nonlinear least-squares fitting routine that graphically represents the autocorrelation function $G(\tau)$ on the ordinate and diffusion time on the abscissa (Fig. 2B). The rate at which GPCRs diffuse within the plasma membrane is reported as the average dwell time (τ_D) of the fluorescence-tagged GPCRs within the observation volume and is calculated from the mid-point of the autocorrelation decay curve. The biphasic autocorrelation curves shown in Fig. 2B are best fit by a two-component model with a very fast component characteristic of the photophysical properties of the fluorescent probe (τ_{D1}) and a slower component representing the translational diffusion of the GPCR within the plasma membrane (τ_{D2}).

Diffusion coefficients for fluorescence-tagged GPCRs in HEK293 cell plasma membranes are reported in Table 1. All diffusion data best fit a two-component model with τ_{D1} values related to the photophysical properties of the fluorescent probe (50–100 μs for YFP and 250–300 μs for GFP) and τ_{D2} values (representing the average dwell time of the GPCR within the observation volume) on the order of 30 milliseconds, yielding a diffusion coefficient on the order of 7.5×10^{-9}cm^2/s. Since FCS measures the mobile fraction of freely diffusing proteins, fluorescence-tagged GPCRs that are sequestered into microdomains with reduced mobility (Day and Kenworthy, 2009) or associated with cytoskeletal or extracellular matrix proteins could photobleach during an FCS recording. In the present study, approximately 40–50% of the initial fluorescence signal was photobleached during the first 10 seconds of each FCS recording (data not shown). This phenomenon, observed for all six GPCRs tested, is consistent with previous results obtained using fluorescence recovery after photobleach (FRAP) to monitor GPCR diffusion (Dorsch et al., 2009; Fonseca and Lambert, 2009).

Figure 2 shows representative FCS autocorrelation graphs for YFP-tagged 5-HT_{2A}, β_2-AR, D_1-dopamine, M_2-muscarinic, dimeric CD-28, and the β_2-AR BiFC pair (β_2-AR/N-YFP + β_2-AR/C-YFP). Inspection of the fluorescence intensity traces in Fig. 2A reveals similar average photon count rates for the GPCR, and the dimeric CD-28/YFP control. The amplitude (y-intercept) of the autocorrelation curve (Fig. 2B) is inversely related to the number of fluorescent proteins or complexes present in the observation volume and is similar for the GPCR and CD-28/YFP. The molecular brightness of the YFP-tagged GPCRs can be determined from the FCS data by dividing the average photon count rate obtained from the fluorescence intensity traces in Fig. 2A (130 kHz on average for the GPCR and for the dimeric CD-28) by the number of fluorescent molecules calculated from the amplitude of the autocorrelation curves in Fig. 2B (using Eq. 4 in the *Materials and Methods* with a 2D FCS model yields and average $N = 10$). This provides an approximate molecular brightness of 13,000 CPSM for the GPCR and dimeric CD-28, consistent with

a dimeric structure for the GPCR. The molecular brightness of the β_2-AR BiFC pair, estimated as 42 kHz (Fig. 2A) divided by 6.3 (the number of molecules determined from Fig. 2B using Eq. 4) is 6667 CPSM, approximately half that of the YFP-tagged GPCR and dimeric CD-28.

PCH analysis uses a 3D Gaussian approximation of the laser beam profile and Poisson statistics to predict what the molecular brightness of the fluorescent particle would be when it is at the center of the observation volume (Chen et al., 1999). PCHs were generated from the FCS data presented in Fig. 2. The shape of the histogram is a function of the number of fluorescent molecules and their molecular brightness, and was the same for the GPCR and dimeric CD-28 (Fig. 3). To generate a histogram, each 10-second fluorescence intensity trace (as in Fig. 2A) was broken down into 1 million 10-μs intervals or bins (PCH bin time = 10 μs). Histograms were constructed in which the number of 10-μs bins was plotted on the y-axis and photon counts were plotted on the x-axis. The resulting histogram depicts the number of bins that registered 1,2,3…n photon counts during one 10-second observation period.

PCHs for the biogenic amine GPCR and dimeric CD-28 (Fig. 3) show an average number of photon counts per 10-μs bin time of 1.25, equivalent to 125,000 counts per second. Dividing by the average number of molecules calculated from the amplitude of the autocorrelation curves in Fig. 2B (using Eq. 4 with a 3D PCH model where $N = 7$) yields an average molecular brightness of 17,857 CPSM for the GPCR and dimeric CD-28. For the β_2-AR BiFC pair, the PCH predicts 0.4 photon counts per 10-μs bin time, equivalent to 40,000 counts per second. Dividing by the average number of molecules calculated from the amplitude of the autocorrelation curve in Fig. 2B (using Eq. 4 with a 3D PCH model where $N = 4.3$) yields an average molecular brightness of 9302 CPSM.

FCS and PCH molecular brightness values for YFP- and GFP-tagged receptors are reported in Table 1. Known monomeric (CD-86) and dimeric (CD-28) plasma membrane receptors with C-terminal GFP (CD-86/GFP and CD-86/GFP-GFP) and YFP (CD-28/YFP) were used to determine the molecular brightness of GFP and YFP monomers and dimers. Molecular brightness values for all GPCRs tested

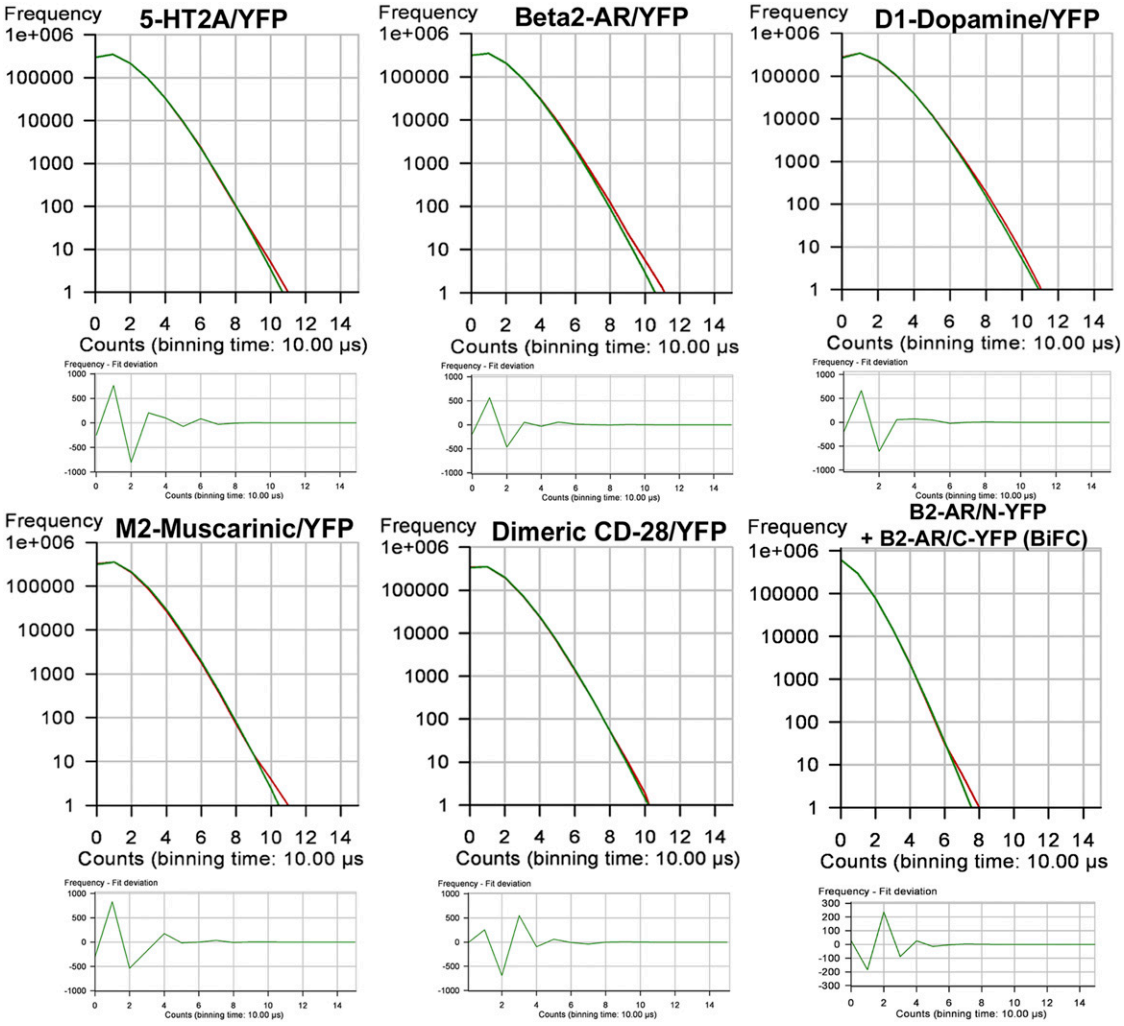

Fig. 3. PCHs of the corresponding FCS recordings shown in Fig. 2. To generate the histograms, each 10-second fluorescence intensity trace (shown in Fig. 2A) was broken down into 1 million 10-μs intervals or bins (PCH bin time = 10 μs). The number of bins is plotted on the y-axis and photon counts on the x-axis. The resulting histogram depicts the number of bins that registered 1,2,3…n photon counts during one 10-second observation period. The residuals of the curve fit (shown in the lower panels) plot the number of bins on the y-axis and photon counts on the x-axis. The data were fit to a one-component model for a single homogenous population of homodimers. The residuals of the curve fit are <2 S.D. and are randomly distributed about zero, indicating that the data are a good fit for the selected model, with reduced χ^2 equal to unity.

were similar to one another and were similar to dimeric CD-28/YFP and tandem GFP attached to monomeric CD-86 (CD-86/GFP-GFP). The monomeric CD-86/GFP control was half the brightness of the dimeric control (Fig. 4) and of the GPCR.

An experimental paradigm using coexpression of fluorescence-tagged GPCRs with an excess of untagged/nonfluorescent receptor was used as an additional measure of GPCR oligomer size. In this paradigm, HEK293 cells were cotransfected with GFP-tagged GPCRs and a 3-fold excess of untagged, nonfluorescent GPCRs. These studies were performed using β_2-AR and M_1-muscarinic receptors. For example, if β_2-AR are monomeric, then coexpression of GFP-tagged β_2-AR with an excess of nonfluorescent β_2-AR would have no effect on the observed molecular brightness. However, if the receptors form homodimers, then this paradigm would produce dimers composed of one GFP-tagged protomer and one nonfluorescent protomer. In this case, the observed molecular brightness would be reduced by half. On the other hand, if the receptors are capable of forming tetramers, then coexpression with a 3-fold excess of untagged receptor should reduce the molecular brightness by greater than 50%. Coexpression of β_2-AR/GFP with excess untagged β_2-AR or M_1/GFP with the excess untagged M_1 receptor reduced the molecular brightness by approximately half. In contrast, coexpression of β_2-AR/GFP with the untagged M_1 receptor had no effect on the molecular brightness of β_2-AR/GFP. These results are consistent with a homodimeric structure for β_2-AR and M_1-muscarinic receptors.

BiFC between the N- and C-YFP attached to the β_2-AR was utilized as an additional control. BiFC involves the recombination of two nonfluorescent halves of a protein, such as the N-YFP and the C-YFP. When two proteins (one with N-YFP and one with C-YFP) are in close proximity, N-YFP and C-YFP can recombine to reconstitute YFP fluorescence. In the present study, YFP BiFC pairs were created using the β_2-AR and A_{2a}-adenosine receptors. Coexpression of β_2-AR/N-YFP with β_2-AR/C-YFP in HEK293 cells results in fluorescence complementation and the generation of YFP fluorescence on the plasma membrane of transfected HEK293 cells (Fig. 5). The specificity of the positive BiFC signal is demonstrated by reduced fluorescence after coexpression of β_2-AR/N-YFP with A_{2a}-adenosine/C-YFP, and restoration of fluorescence in cells coexpressing A_{2a}-adenosine/N-YFP with A_{2a}-adenosine/C-YFP.

Plasma membrane FCS analysis of cells coexpressing β_2-AR/N-YFP and β_2-AR/C-YFP yielded diffusion coefficients

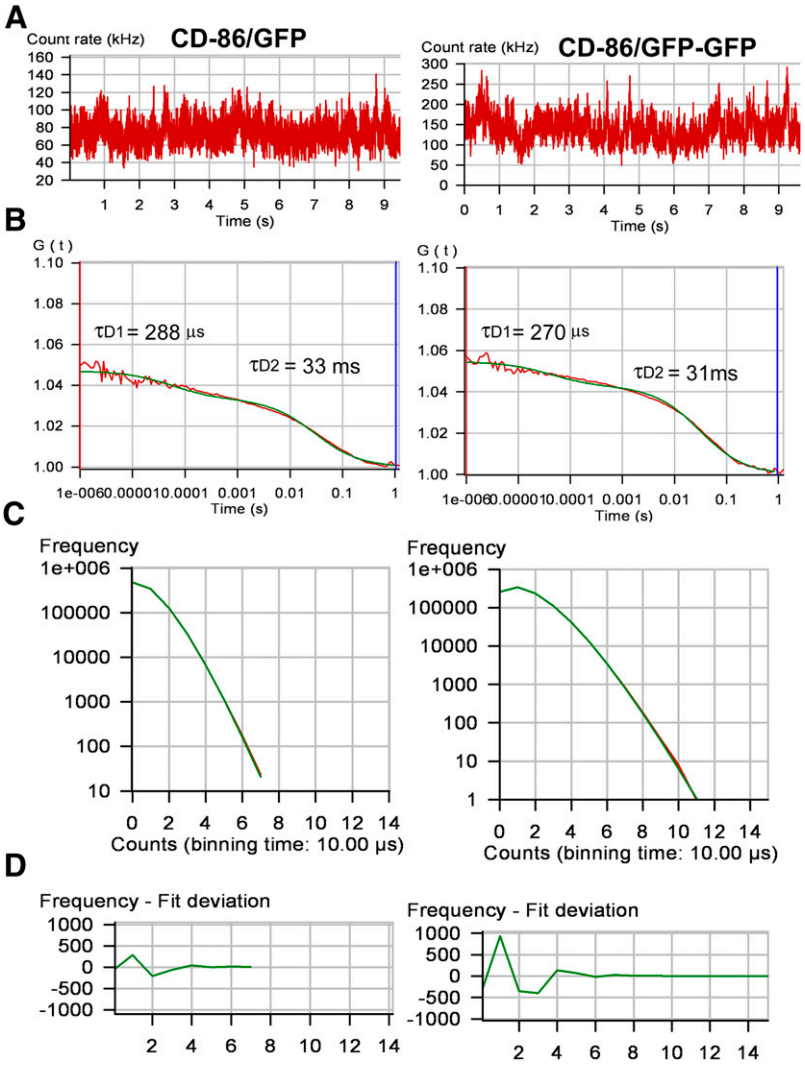

Fig. 4. FCS recordings from the plasma membrane of HEK293 cells expressing CD-86/GFP and CD-86/GFP-GFP. (A) Fluorescence intensity traces for one 10-second observation period. (B) Autocorrelation analysis of the fluorescence intensity traces. The red line represents the autocorrelation of the observed fluorescence signal and the green line represents the fit to a two-component model. The fast component (measured in microseconds) is related to the photophysical properties of the fluorescent probe, whereas the slower component (measured in milliseconds) represents the translational diffusion of the fluorescence-tagged receptors in the plasma membrane. (C) PCHs of the corresponding FCS recordings yield molecular brightness values of 9693 CPSM for CD-86/GFP and 18,194 CPSM for CD-86/GFP-GFP. (D) Residuals of the curve fit. The data were fit to a one-component model for a single homogenous population of fluorescence-tagged receptors.

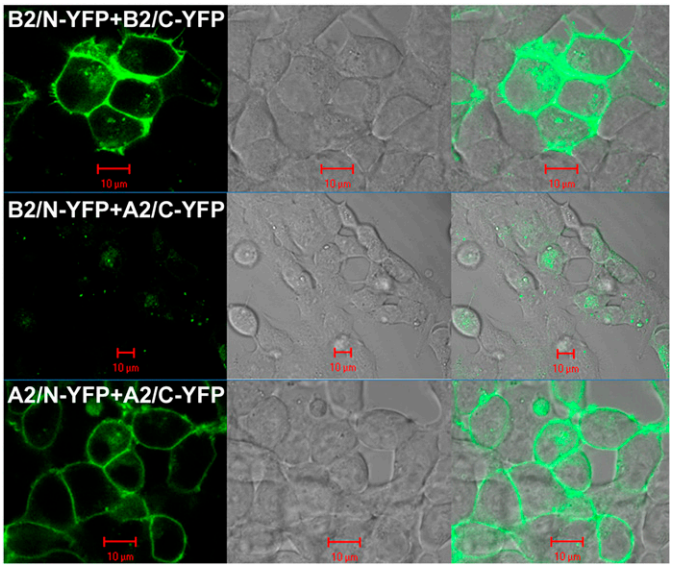

Fig. 5. BiFC. The N- and C-terminal halves of YFP were attached to the C-terminal end of β_2-AR or A_{2a}-adenosine receptors. (Top) HEK293 cells coexpressing β_2-AR/N-YFP with β_2-AR/C-YFP show plasma membrane YFP fluorescence 20 hour post-transfection (left). The middle panel shows the differential interference contrast image and the right panel shows the merged image. (Middle) HEK293 cells coexpressing β_2-AR/N-YFP and A_{2a}-adenosine/C-YFP show minimal fluorescence complementation. (Bottom) Restoration of plasma membrane fluorescence complementation in HEK293 cells coexpressing A_{2a}-adenosine/N-YFP and A_{2a}-adenosine/C-YFP. Red scale bar, 10 μm.

similar to those observed for the parent β_2-AR/YFP complex (Table 1). If β_2-AR form homodimers, then the molecular brightness of the β_2-AR BiFC pair would be expected to be approximately half that observed for β_2-AR/YFP. FCS and PCH analyses revealed molecular brightness values for the β_2-AR BiFC pair that were approximately half that observed for β_2-AR/YFP and the dimeric CD-28/YFP control (Table 1), again predicting a homodimeric structure for the β_2-AR.

Molecular brightness values equivalent to a homodimer, as reported in Table 1, could be produced by a homogeneous population of homodimers or by a mixture of monomers, dimers and tetramers. Since FCS analysis would yield similar results in both cases (Meseth et al., 1999), PCH and reduced χ^2 analyses were used to determine the goodness of fit to both one and multicomponent models (Müller et al., 2000). Reduced χ^2 values were close to unity when the PCH data were fit to a one-component model for a homogeneous population of homodimers (Table 1). Multicomponent modeling of the PCH data to test for a mixture of monomers, dimers and tetramers did not provide a better fit of the data. Modeling the data using fixed monomer/dimer/tetramer ratios of 20%/70%/10% and 40%/40%/20% (ratios predicted to give an average molecular brightness equivalent to a dimer) produced reduced χ^2 values greater than 3 and 10, respectively (Figs. 6 and 7).

To determine the effect of agonist treatment on receptor diffusion rate and on GPCR oligomer status, transfected cells expressing GFP-tagged β_2-AR or M_1-muscarinic receptors were treated with 0.1 μM isoproterenol or carbachol, respectively, for 1 minute prior to FCS recording. As shown in Table 2, diffusion rates and molecular brightness values were not altered after treatment with agonist, similar to our previous findings with serotonin 5-HT_{2C} receptors (Herrick-Davis et al., 2012).

The FCS data presented in Table 2 evaluate the relationship between molecular brightness and receptor expression level for β_2-AR and M_1-muscarinic receptors. The surface area of plasma membrane in the observation volume and the number of dimers per cell were calculated as described in the *Materials and Methods*. There was no evidence of dimers dissociating into monomers or associating into tetramers over a 10-fold range of receptor expression level. Similar results were obtained for all GPCRs tested in this study.

Discussion

The present study was preformed to shed light on the ongoing controversy related to class A GPCR oligomer size. Confocal microscopy-based FCS was chosen as the method of analysis based on its sensitivity and applicability to live cell membranes. FCS records the fluctuations in fluorescence intensity arising from individual fluorescent molecules, or in this case fluorescence-tagged GPCRs, as they diffuse through the plasma membrane. Two different fluorescent probes were used to ensure that the results were not due to a unique photophysical property of the fluorescent probe and to determine reproducibility of results. Diffusion coefficients for the biogenic amine receptors on the order of 7.5×10^{-9} cm^2/s are similar to previously published diffusion coefficients for class A GPCRs (reviewed in Briddon and Hill, 2007). The diffusion rate of a membrane protein is related to the cubic root of the protein's mass, such that an 8-fold change in mass would be required to produce a 2-fold change in the diffusion rate. To be resolved by FCS, the diffusion rates of two proteins must differ by a factor of 1.6 or greater (Meseth et al., 1999). Therefore, GPCR monomers, dimers, and tetramers cannot be distinguished from one another based on their diffusion coefficients alone.

Information about a protein's oligomer size can be obtained by analyzing the amplitude of the fluorescence intensity fluctuations recorded during an FCS experiment and generating a PCH to determine the molecular brightness (Chen et al., 1999). Since the molecular brightness is proportional to the number of fluorescent molecules traveling together within a protein complex, a GPCR monomer with a single fluorescent tag would have a molecular brightness of x, a dimer carrying two fluorescent tags would be 2x, a tetramer would be 4x, and so forth. PCH analysis revealed similar molecular brightness values for all six GPCRs tested. Molecular brightness values were similar to the dimeric controls and twice the monomeric controls, consistent with a dimeric structure for the biogenic amine GPCR. Two additional plasma membrane controls were utilized using BiFC constructs and coexpression with excess untagged/nonfluorescent receptors. In both cases, the results were consistent with a homodimeric structure for the biogenic amine GPCR examined in this study.

Previous studies designed to assess the oligomer status of the biogenic amine GPCR have utilized a variety of techniques, including RET, FLIM, FRAP, total internal reflection fluorescence (TIRF), and FCS. These methods differ in sensitivity and the population of receptors that they examine. RET and FLIM are proximity assays, whereas TIRF and FCS have near single molecule sensitivity. TIRF, FRAP, and FCS measure the mobile fraction of receptors and allow discrete regions of plasma membrane to be evaluated, whereas BRET measures the entire pool of receptors. In terms of determining

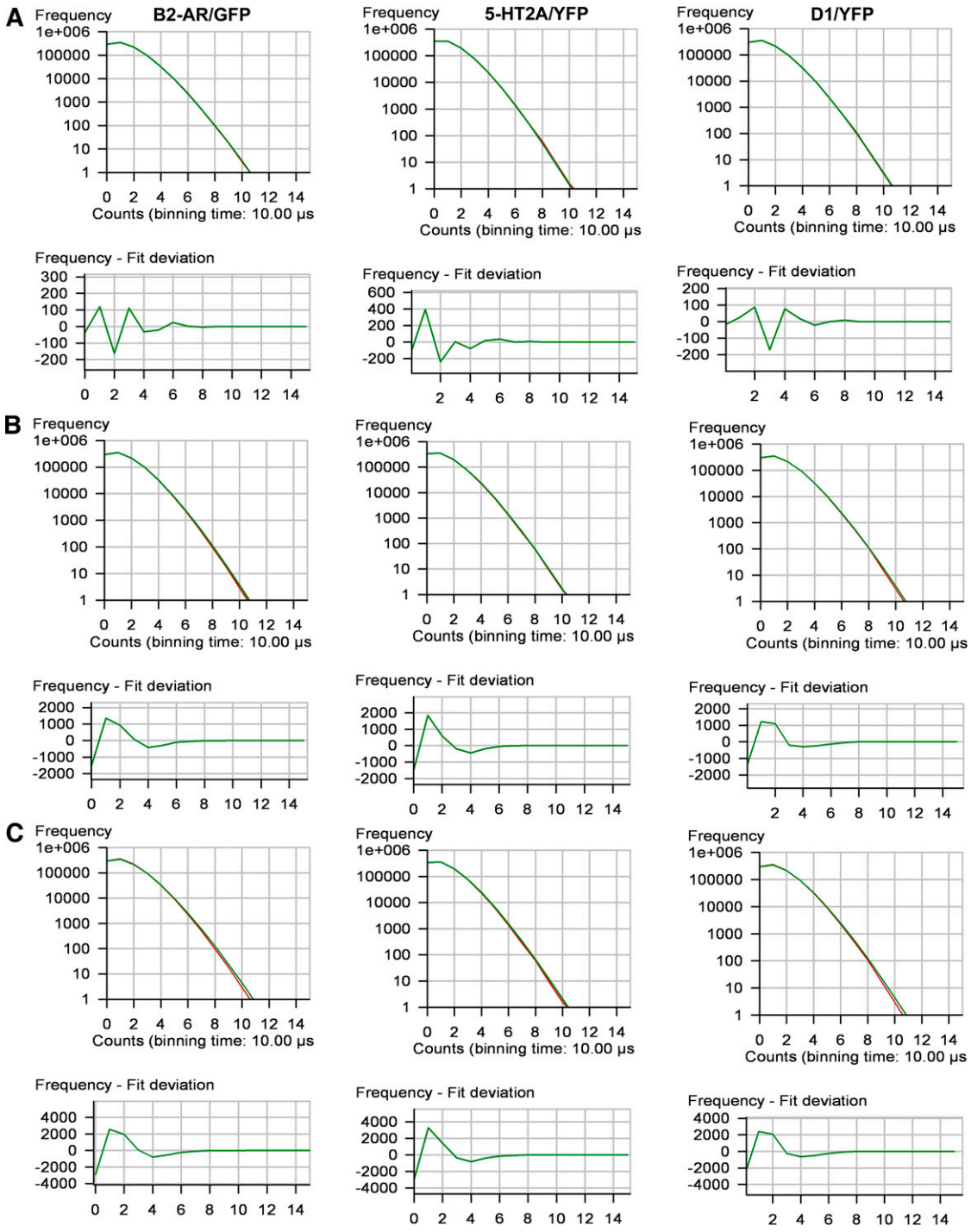

Fig. 6. Single-component and multicomponent analyses for HEK293 cells expressing β_2-AR/GFP, 5-HT_{2A}/YFP, or D_1/YFP. PCHs and residuals of the curve fit for the following: (A) a one-component fit of the data for a single population of fluorescence-tagged receptors; (B) a mixture of monomers/dimers/tetramers in a fixed 20%/70%/10% ratio; and (C) a mixture of monomers/dimers/tetramers in a fixed 40%/40%/20% ratio. Reduced χ^2 values for the one-component and the multicomponent 20%70%/10% and 40%/40%/20% ratios were 0.8, 4.7, and 18, respectively, for β_2-AR/GFP; 1.1, 4.3, and 17, respectively, for 5-HT_{2A}/YFP; and 1.0, 4.6, and 18, respectively, for D_1/YFP.

oligomer number, the above-described methods have produced conflicting results even within the same biogenic amine receptor subfamily. For example, RET, FRAP, and TIRF studies of M_1-, M_2-, and M_3-muscarinic receptors have reported monomers (Hern et al., 2010), dimers (Goin and Nathanson, 2006; Hern et al., 2010; Patowary et al., 2013), and tetramers (Pisterzi et al., 2010; McMillin et al., 2011; Patowary et al., 2013). RET and FRAP studies of β_1-AR and β_2-AR have reported monomers (James et al., 2006; Dorsch et al., 2009), dimers (Mercier et al., 2002; Dorsch et al., 2009), and higher-order oligomers (Dorsch et al., 2009; Fung et al., 2009). D_1- and D_2-dopamine receptors have been reported to form homodimers and higher-order oligomers assayed by RET (Guo et al., 2008) and using a nuclear translocation assay

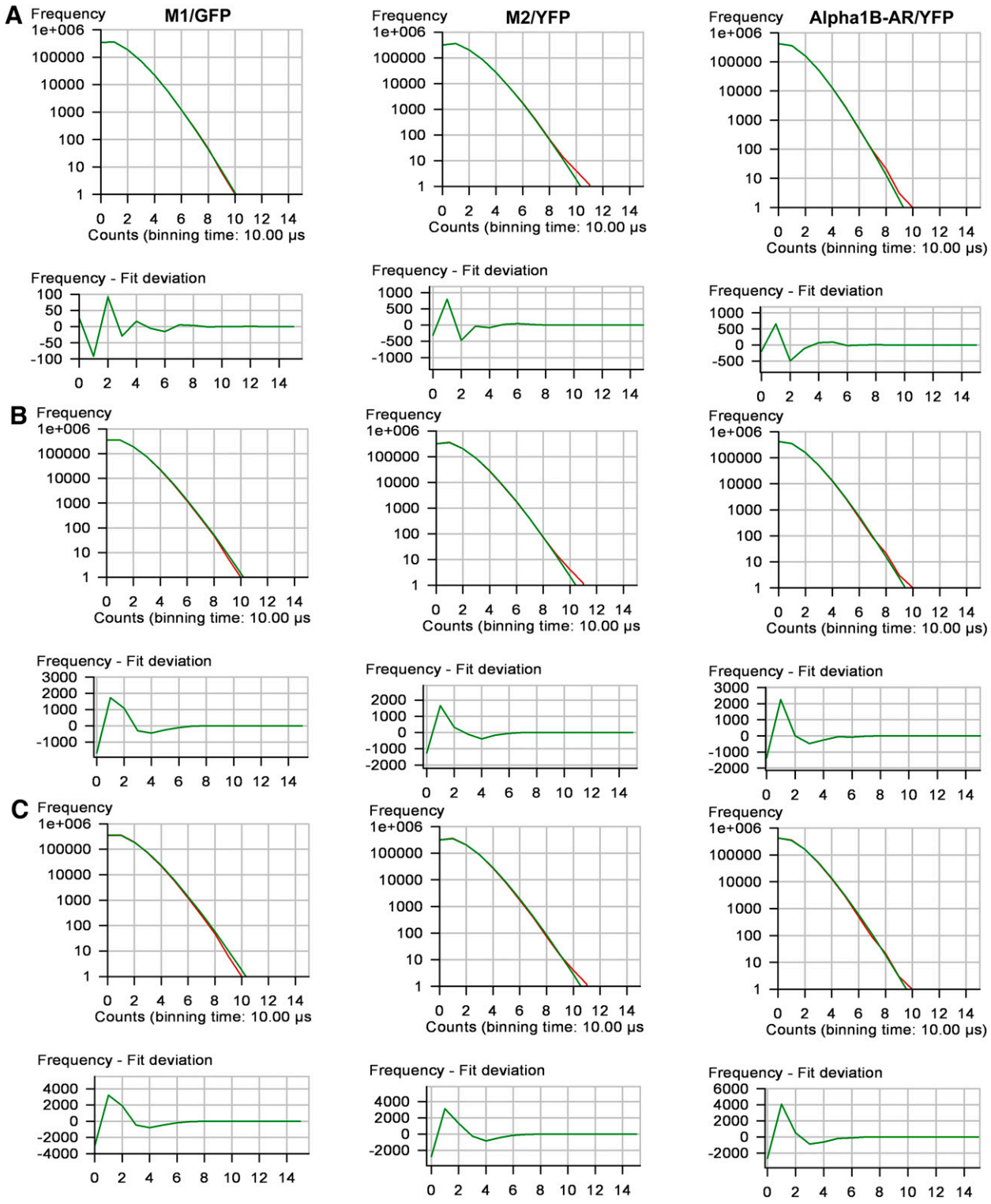

Fig. 7. Single-component and multicomponent analyses for HEK293 cells expressing M_1/GFP, M_2/YFP or α_{1b}-AR/YFP. PCH and residuals of the curve fit for the following: (A) a one-component fit of the data for a single population of fluorescence-tagged receptors; (B) a mixture of monomers/dimers/tetramers in a fixed 20%/70%/10% ratio; and (C) a mixture of monomers/dimers/tetramers in a fixed 40%/40%/20% ratio. Reduced χ^2 values for the one-component and the multicomponent 20%/70%/10% and 40%/40%/20% ratios were 0.7, 7.0 and 23, respectively, for M_1/GFP; 1.1, 3.2 and 16, respectively, for M_2/YFP; and 1.3, 6.0 and 23, respectively, for α_{1b}-AR/YFP.

(O'Dowd et al., 2011). RET studies of serotonin 5-HT_{1A} receptors have reported homodimers (Kobe et al., 2008) and higher-order oligomers (Ganguly et al., 2011), whereas 5-HT_{2A}, 5-HT_{2C}, 5-HT_4, and 5-HT_7 appear to be predominantly dimeric (Herrick-Davis et al., 2005, 2012; Brea et al., 2009; Pellissier et al., 2011; Teitler and Klein, 2012). To further complicate the issue, FRAP and TIRF studies suggested that β_1-AR and M_1-muscarinic receptors may exist in equilibrium

TABLE 2

Relationship between molecular brightness and receptor expression level

Plasma membrane 2D FCS molecular brightness analysis of HEK293 cells expressing different levels of GFP-tagged M_1-muscarinic receptors (M_1/GFP), β_2-adrenergic receptors (β_2-AR/GFP), and monomeric CD-86 labeled with two GFP tags (CD-86/GFP-GFP). The photon count rate (kHz) is a measure of the overall fluorescence intensity of the region of plasma membrane in the observation volume and n is the number of receptor dimers in the observation volume (calculated as in Eq. 4). Molecular brightness values are reported as photon counts per molecule. Data represent the mean ± S.E.M. from three cells with similar photon count rates (kHz). The area of plasma membrane in the observation volume was calculated using $\pi{\omega_0}^2$, where ω_0 is the radius of the observation volume (calculated as in the *Materials and Methods*), and was used to determine the number of dimers per μm^2 of plasma membrane. An HEK293 cell total surface area equivalent to 2591 μm^2 (Sommerhage et al., 2008) was used to estimate the total number of dimers per cell.

Receptor	Count Rate	n	Molecular Brightness	Dimers	
	kHz			*per μm^2*	*per cell*
M_1/GFP	37 ± 1.7	3.0 ± 0.2	12,525 ± 244	10	2.6×10^4
β_2-AR/GFP	46 ± 4.4	3.5 ± 0.5	13,083 ± 941	12	3.1×10^4
CD-86/GFP-GFP	69 ± 12	5.6 ± 1.2	12,537 ± 595	20	5.2×10^4
M_1/GFP	113 ± 2.9	8.9 ± 0.4	12,797 ± 446	31	8.0×10^4
β_2-AR/GFP	192 ± 8.8	15 ± 0.4	12,579 ± 465	53	1.4×10^5
M_1/GFP	206 ± 7.4	16 ± 0.2	12,460 ± 704	56	1.5×10^5
CD-86/GFP-GFP	223 ± 12	18 ± 0.7	12,750 ± 233	63	1.6×10^5
β_2-AR/GFP	311 ± 26	26 ± 2.7	12,137 ± 324	91	2.4×10^5
M_1/GFP	358 ± 4.5	29 ± 1.2	12,496 ± 707	102	2.6×10^5
β_2-AR/GFP	413 ± 19	34 ± 1.0	11,970 ± 285	119	3.1×10^5

between monomeric and dimeric states (Dorsch et al., 2009; Hern et al., 2010). In addition, mixed populations of homodimers and higher-order oligomers for D_1- and D_2-dopamine and M_3-muscarinic receptors have been reported (Fonseca and Lambert, 2009; O'Dowd et al., 2011; Patowary et al., 2013). Our FCS/PCH studies did not reveal the presence of tetramers or higher-order oligomers of biogenic amine receptors on the plasma membrane. PCH provides an estimate of the average molecular brightness of all fluorescent species present in the sample (Müller et al., 2000); thus, if the GPCRs tested in this study exist in monomer-dimer or dimer-tetramer equilibrium, then the observed molecular brightness values would be an average based on the monomer-dimer or dimer-tetramer composition of the sample. Reduced χ^2 analysis of a multicomponent fit of the PCH data, testing for the presence of a mixture of monomers, dimers, and tetramers, did not provide a better fit of the data than a one-component analysis for a homogeneous population of homodimers.

Attempts to reconcile differences in GPCR oligomer status reported by the different methods used in the literature have led to the suggestion that receptor expression level may influence GPCR monomer-dimer and/or dimer-tetramer states on the plasma membrane, with low expression levels favoring monomeric forms and higher expression levels favoring association of dimers into tetramers (Hern et al., 2010; Lambert, 2010; Patowary et al., 2013). In the present study, we compared the molecular brightness of fluorescence-tagged GPCRs over a 10-fold range of receptor expression levels. FCS analysis of the mobile fraction of plasma membrane receptors demonstrates that the homodimer configuration is maintained from 26,000 dimers per cell to 310,000 dimers per cell. Because the FCS technique is best suited for studying proteins at low expression levels, we cannot rule out the possibility that significantly higher expression levels may lead to receptor clustering. It is recognized that palmitoylation promotes sequestration of GPCRs into discrete microdomains (Kobe et al., 2008; Day and Kenworthy, 2009; Woehler et al., 2009), and that the majority of class A GPCRs have at least one palmitoylation site in the C terminus following helix 8. Receptor clustering into membrane microdomains would increase local receptor concentrations, complicating the interpretation of RET-based studies that monitor protein proximity, because positive RET is suggestive of but does not demonstrate protein–protein interaction. Further complicating the issue, stochastic RET has been reported for receptors clustered in membrane microdomains (Meyer et al., 2006; Kobe et al., 2008; Woehler et al., 2009). In one study, serotonin 5-HT_{1A} receptors clustered in membrane microdomains gave RET values consistent with an oligomer number greater than 2, whereas nonpalmitoylated mutant receptors that were excluded from microdomains gave an oligomer number of 2 (Woehler et al., 2009). It is interesting to note that studies employing techniques with near single molecule sensitivity (TIRF and FCS) have only reported monomers or dimers, without tetramers or higher-order oligomers (Hern et al., 2010; Kasai et al., 2011; Herrick-Davis et al., 2012), as observed in the present study.

Studies examining the effect of ligands on GPCR oligomer status have produced differing results ranging from no effect to dissociation or association of dimers into oligomers. fluorescence RET/FLIM studies of serotonin 5-HT_{1A} receptors (Kobe et al., 2008) and FCS studies of 5-HT_{2C} receptors (Herrick-Davis et al., 2012), along with FRAP studies of β_1-AR and β_2-AR (Dorsch et al., 2009) and fluorescence RET studies of M_1- and M_2-muscarinic receptors (Goin et al., 2006), report no effect of agonist on GPCR homodimer/oligomer status in intact cells. On the other hand, studies of 5-HT1A (Ganguly et al., 2011), β_2-AR (Fung et al., 2009), M_3-muscarinic (Alvarez-Curto et al., 2010), and D_1- and D_2-dopamine receptors (Guo et al., 2008; O'Dowd et al., 2011) suggest that these receptors form tetramers or higher-order oligomers that are differentially regulated by treatment with various ligands. It is probable that the reported changes in GPCR dimer/oligomer status after ligand treatment are method, ligand, and receptor dependent. In our FCS studies, treatment with isoproterenol or carbachol did not result in β_2-AR or M_1-muscarinic homodimer dissociation or association into higher-order oligomers. Since FCS measures mobile proteins, we cannot exclude the possibility that agonist binding enhances GPCR sequestration and possible clustering within membrane microdomains with reduced mobility (Day and Kenworthy, 2009). GPCR trafficking between mobile and less

mobile fractions could potentially account for some of the variability obtained with different techniques that monitor different fractions or subpopulations of receptors within the plasma membrane.

In summary, the functional significance of homodimerization for class A GPCRs is still a subject of great debate. It is possible that homodimerization is an essential step in protein folding required for exit from the endoplasmic reticulum (Salahpour et al., 2004; Herrick-Davis et al., 2006; Lopez-Gimenez et al., 2007) because the dimer may represent the minimal functional signaling unit. In the present study, the enhanced sensitivity of FCS over proximity-based assays provides conclusive demonstration of the presence of biogenic amine homodimers, and lack of tetramers or higher-order complexes, freely diffusing within the plasma membrane of living cells. The homodimer structure was not altered by receptor expression level or after agonist binding, consistent with the hypothesis that the homodimer represents the basic signaling unit.

Authorship Contributions

Participated in research design: Herrick-Davis, Grinde, Cowan, Mazurkiewicz.

Conducted experiments: Herrick-Davis, Grinde, Mazurkiewicz.

Contributed new reagents or analytic tools: Cowan.

Performed data analysis: Herrick-Davis, Mazurkiewicz.

Wrote or contributed to the writing of the manuscript: Herrick-Davis, Grinde, Cowan, Mazurkiewicz.

References

Albizu L, Cottet M, Kralikova M, Stoev S, Seyer R, Brabet I, Roux T, Bazin H, Bourrier E, and Lamarque L et al. (2010) Time-resolved FRET between GPCR ligands reveals oligomers in native tissues. *Nat Chem Biol* **6**:587–594.

Alvarez-Curto E, Ward RJ, Pediani JD, and Milligan G (2010) Ligand regulation of the quaternary organization of cell surface M3 muscarinic acetylcholine receptors analyzed by fluorescence resonance energy transfer (FRET) imaging and homogeneous time-resolved FRET. *J Biol Chem* **285**:23318–23330.

Brea J, Castro M, Giraldo J, López-Giménez JF, Padín JF, Quintián F, Cadavid MI, Vilaró MT, Mengod G, and Berg KA et al. (2009) Evidence for distinct antagonist-revealed functional states of 5-hydroxytryptamine(2A) receptor homodimers. *Mol Pharmacol* **75**:1380–1391.

Briddon SJ and Hill SJ (2007) Pharmacology under the microscope: the use of fluorescence correlation spectroscopy to determine the properties of ligand-receptor complexes. *Trends Pharmacol Sci* **28**:637–645.

Canals M, Burgueño J, Marcellino D, Cabello N, Canela EI, Mallol J, Agnati L, Ferré S, Bouvier M, and Fuxe K et al. (2004) Homodimerization of adenosine A2A receptors: qualitative and quantitative assessment by fluorescence and bioluminescence energy transfer. *J Neurochem* **88**:726–734.

Chen Y, Müller JD, So PT, and Gratton E (1999) The photon counting histogram in fluorescence fluctuation spectroscopy. *Biophys J* **77**:553–567.

Chen Y, Wei LN, and Müller JD (2003) Probing protein oligomerization in living cells with fluorescence fluctuation spectroscopy. *Proc Natl Acad Sci USA* **100**: 15492–15497.

Cole RW, Jinadasa T, and Brown CM (2011) Measuring and interpreting point spread functions to determine confocal microscope resolution and ensure quality control. *Nat Protoc* **6**:1929–1941.

Day CA and Kenworthy AK (2009) Tracking microdomain dynamics in cell membranes. *Biochim Biophys Acta* **1788**:245–253.

Digman MA, Brown CM, Sengupta P, Wiseman PW, Horwitz AR, and Gratton E (2005) Measuring fast dynamics in solutions and cells with a laser scanning microscope. *Biophys J* **89**:1317–1327.

Dorsch S, Klotz KN, Engelhardt S, Lohse MJ, and Bünemann M (2009) Analysis of receptor oligomerization by FRAP microscopy. *Nat Methods* **6**:225–230.

Fonseca JM and Lambert NA (2009) Instability of a class a G protein-coupled receptor oligomer interface. *Mol Pharmacol* **75**:1296–1299.

Fotiadis D, Liang Y, Filipek S, Saperstein DA, Engel A, and Palczewski K (2003) Atomic-force microscopy: Rhodopsin dimers in native disc membranes. *Nature* **421**:127–128.

Fung JJ, Deupi X, Pardo L, Yao XJ, Velez-Ruiz GA, Devree BT, Sunahara RK, and Kobilka BK (2009) Ligand-regulated oligomerization of beta(2)-adrenoceptors in a model lipid bilayer. *EMBO J* **28**:3315–3328.

Ganguly S and Chattopadhyay A (2010) Cholesterol depletion mimics the effect of cytoskeletal destabilization on membrane dynamics of the serotonin1A receptor: A zFCS study. *Biophys J* **99**:1397–1407.

Ganguly S, Clayton AH, and Chattopadhyay A (2011) Organization of higher-order oligomers of the serotonin$_{1A}$(A) receptor explored utilizing homo-FRET in live cells. *Biophys J* **100**:361–368.

Goin JC and Nathanson NM (2006) Quantitative analysis of muscarinic acetylcholine receptor homo- and heterodimerization in live cells: regulation of receptor down-regulation by heterodimerization. *J Biol Chem* **281**:5416–5425.

Guo W, Urizar E, Kralikova M, Mobarec JC, Shi L, Filizola M, and Javitch JA (2008) Dopamine D2 receptors form higher order oligomers at physiological expression levels. *EMBO J* **27**:2293–2304.

Harikumar KG, Happs RM, and Miller LJ (2008) Dimerization in the absence of higher-order oligomerization of the G protein-coupled secretin receptor. *Biochim Biophys Acta* 1778:2555–2563.

Hern JA, Baig AH, Mashanov GI, Birdsall B, Corrie JET, Lazareno S, Molloy JE, and Birdsall NJM (2010) Formation and dissociation of M1 muscarinic receptor dimers seen by total internal reflection fluorescence imaging of single molecules. *Proc Natl Acad Sci USA* **107**:2693–2698.

Herrick-Davis K, Grinde E, Harrigan TJ, and Mazurkiewicz JE (2005) Inhibition of serotonin 5-hydroxytryptamine2c receptor function through heterodimerization: receptor dimers bind two molecules of ligand and one G-protein. *J Biol Chem* **280**: 40144–40151.

Herrick-Davis K, Weaver BA, Grinde E, and Mazurkiewicz JE (2006) Serotonin 5-HT$_{2C}$ receptor homodimer biogenesis in the endoplasmic reticulum: real-time visualization with confocal fluorescence resonance energy transfer. *J Biol Chem* **281**:27109–27116.

Herrick-Davis K, Grinde E, and Weaver BA (2007) Serotonin 5-HT(2C) receptor homodimerization is not regulated by agonist or inverse agonist treatment. *Eur J Pharmacol* **568**:45–53.

Herrick-Davis K, Grinde E, Lindsley T, Cowan A, and Mazurkiewicz JE (2012) Oligomer size of the serotonin 5-hydroxytryptamine 2C (5-HT2C) receptor revealed by fluorescence correlation spectroscopy with photon counting histogram analysis: evidence for homodimers without monomers or tetramers. *J Biol Chem* **287**: 23604–23614.

James JR, Oliveira MI, Carmo AM, Iaboni A, and Davis SJ (2006) A rigorous experimental framework for detecting protein oligomerization using bioluminescence resonance energy transfer. *Nat Methods* **3**:1001–1006.

Jastrzebska B, Ringler P, Palczewski K, and Engel A (2013) The rhodopsin-transducin complex houses two distinct rhodopsin molecules. *J Struct Biol* **182**: 164–172.

Kasai RS, Suzuki KGN, Prossnitz ER, Koyama-Honda I, Nakada C, Fujiwara TK, and Kusumi A (2011) Full characterization of GPCR monomer-dimer dynamic equilibrium by single molecule imaging. *J Cell Biol* **192**:463–480.

Kilpatrick LE, Briddon SJ, and Holliday ND (2012) Fluorescence correlation spectroscopy, combined with bimolecular fluorescence complementation, reveals the effects of β-arrestin complexes and endocytic targeting on the membrane mobility of neuropeptide Y receptors. *Biochim Biophys Acta* **1823**:1068–1081.

Kobe F, Renner U, Woehler A, Wlodarczyk J, Papusheva E, Bao G, Zeug A, Richter DW, Neher E, and Ponimaskin E (2008) Stimulation- and palmitoylation-dependent changes in oligomeric conformation of serotonin 5-HT1A receptors. *Biochim Biophys Acta* **1783**:1503–1516.

Knepp AM, Periole X, Marrink SJ, Sakmar TP, and Huber T (2012) Rhodopsin forms a dimer with cytoplasmic helix 8 contacts in native membranes. *Biochemistry* **51**: 1819–1821.

Lambert NA (2010) GPCR dimers fall apart. *Sci Signal* **3**:pe12.

Liu P, Sudhaharan T, Koh RM, Hwang LC, Ahmed S, Maruyama IN, and Wohland T (2007) Investigation of the dimerization of proteins from the epidermal growth factor receptor family by single wavelength fluorescence cross-correlation spectroscopy. *Biophys J* **93**:684–698.

Lopez-Gimenez JF, Canals M, Pediani JD, and Milligan G (2007) The alpha1b-adrenoceptor exists as a higher-order oligomer: effective oligomerization is required for receptor maturation, surface delivery, and function. *Mol Pharmacol* 71:1015–1029.

Malengo G, Andolfo A, Sidenius N, Gratton E, Zamai M, and Caiolfa VR (2008) Fluorescence correlation spectroscopy and photon counting histogram on membrane proteins: functional dynamics of the glycosylphosphatidylinositol-anchored urokinase plasminogen activator receptor. *J Biomed Opt* **13**:031215.

Magde D, Elson E, and Webb WW (1972) Thermodynamic fluctuations in a reacting system: measurement by fluorescence correlation spectroscopy. *Phys Rev Lett* **29**:705–708.

McMillin SM, Heusel M, Liu T, Costanzi S, and Wess J (2011) Structural basis of M_3 muscarinic receptor dimer/oligomer formation. *J Biol Chem* **286**:28584–28598.

Mercier JF, Salahpour A, Angers S, Breit A, and Bouvier M (2002) Quantitative assessment of beta 1- and beta 2-adrenergic receptor homo- and heterodimerization by bioluminescence resonance energy transfer. *J Biol Chem* **277**:44925–44931.

Meseth U, Wohland T, Rigler R, and Vogel H (1999) Resolution of fluorescence correlation measurements. *Biophys J* **76**:1619–1631.

Meyer BH, Segura JM, Martinez KL, Hovius R, George N, Johnsson K, and Vogel H (2006) FRET imaging reveals that functional neurokinin-1 receptors are monomeric and reside in membrane microdomains of live cells. *Proc Natl Acad Sci USA* **103**:2138–2143.

Milligan G (2013) The prevalence, maintenance, and relevance of g protein-coupled receptor oligomerization. *Mol Pharmacol* **84**:158–169.

Müller JD, Chen Y, and Gratton E (2000) Resolving heterogeneity on the single molecular level with the photon-counting histogram. *Biophys J* **78**:474–486.

Neugart F, Zappe A, Buk DM, Ziegler I, Steinert S, Schumacher M, Schopf E, Bessey R, Wurster K, and Tietz C et al. (2009) Detection of ligand-induced CNTF receptor dimers in living cells by fluorescence cross correlation spectroscopy. *Biochim Biophys Acta* **1788**:1890–1900.

O'Dowd BF, Ji X, Alijaniaram M, Nguyen T, and George SR (2011) Separation and reformation of cell surface dopamine receptor oligomers visualized in cells. *Eur J Pharmacol* **658**:74–83.

Patel RC, Kumar U, Lamb DC, Eid JS, Rocheville M, Grant M, Rani A, Hazlett T, Patel SC, and Gratton E et al. (2002) Ligand binding to somatostatin receptors induces receptor-specific oligomer formation in live cells. *Proc Natl Acad Sci USA* **99**:3294–3299.

Patowary S, Alvarez-Curto E, Xu TR, Holz JD, Oliver JA, Milligan G, and Raicu V (2013) The muscarinic M3 acetylcholine receptor exists as two differently sized complexes at the plasma membrane. *Biochem J* **452**:303–312.

Pellissier LP, Barthet G, Gaven F, Cassier E, Trinquet E, Pin JP, Marin P, Dumuis A, Bockaert J, and Banères JL et al. (2011) G protein activation by serotonin type 4 receptor dimers: evidence that turning on two protomers is more efficient. *J Biol Chem* **286**:9985–9997.

Pisterzi LF, Jansma DB, Georgiou J, Woodside MJ, Chou JT, Angers S, Raizu V, and Wells JW (2010) Oligomeric size of the M_2 muscarinic receptor in live cells as determined by quantitative fluorescence resonance energy transfer. *J Biol Chem* 285:16723–16738.

Pramanik A, Olsson M, Langel U, Bartfai T, and Rigler R (2001) Fluorescence correlation spectroscopy detects galanin receptor diversity on insulinoma cells. *Biochemistry* **40**:10839–10845.

Qian H and Elson EL (1991) Analysis of confocal laser-microscope optics for 3-D fluorescence correlation spectroscopy. *Appl Opt* **30**:1185–1195.

Rashid AJ, So CH, Kong MM, Furtak T, El-Ghundi M, Cheng R, O'Dowd BF, and George SR (2007) D1-D2 dopamine receptor heterooligomers with unique pharmacology are coupled to rapid activation of Gq/11 in the striatum. *Proc Natl Acad Sci USA* **104**:654–659.

Rigler R, Mets U, Widengren J, and Kask P (1993) Fluorescence correlation spectroscopy with high count rate and low background: analysis of translational diffusion. *Eur Biophys J* **22**:169–175.

Saffarian S, Li Y, Elson EL, and Pike LJ (2007) Oligomerization of the EGF receptor investigated by live cell fluorescence intensity distribution analysis. *Biophys J* **93**: 1021–1031.

Salahpour A, Angers S, Mercier JF, Lagacé M, Marullo S, and Bouvier M (2004) Homodimerization of the beta2-adrenergic receptor as a prerequisite for cell surface targeting. *J Biol Chem* **279**:33390–33397.

Savatier J, Jalaguier S, Ferguson ML, Cavaillès V, and Royer CA (2010) Estrogen receptor interactions and dynamics monitored in live cells by fluorescence cross-correlation spectroscopy. *Biochemistry* **49**:772–781.

Sommerhage F, Helpenstein R, Rauf A, Wrobel G, Offenhäusser A, and Ingebrandt S (2008) Membrane allocation profiling: a method to characterize three-dimensional cell shape and attachment based on surface reconstruction. *Biomaterials* **29**: 3927–3935.

Teitler M and Klein MT (2012) A new approach for studying GPCR dimers: drug-induced inactivation and reactivation to reveal GPCR dimer function in vitro, in primary culture, and in vivo. *Pharmacol Ther* **133**:205–217.

Ulbrich MH and Isacoff EY (2007) Subunit counting in membrane-bound proteins. *Nat Methods* **4**:319–321.

Woehler A, Wlodarczyk J, and Ponimaskin EG (2009) Specific oligomerization of the 5-HT1A receptor in the plasma membrane. *Glycoconj J* **26**:749–756.

Whorton MR, Bokoch MP, Rasmussen SG, Huang B, Zare RN, Kobilka B, and Sunahara RK (2007) A monomeric G protein-coupled receptor isolated in a high-density lipoprotein particle efficiently activates its G protein. *Proc Natl Acad Sci USA* **104**:7682–7687.

Zacharias DA, Violin JD, Newton AC, and Tsien RY (2002) Partitioning of lipid-modified monomeric GFPs into membrane microdomains of live cells. *Science* **296**: 913–916.

Address correspondence to: Dr. Katharine Herrick-Davis, Center for Neuropharmacology and Neuroscience, Albany Medical College, 47 New Scotland Ave., Mail Code 136, Albany, NY 12208. E-mail: daviskh@mail.amc.edu